

MHD Equilibrium of Heliotron J Plasmas

SUZUKI Yasuhiro, NAKAMURA Yuji, KONDO Katsumi,
NAKAJIMA Noriyoshi¹ and HAYASHI Takaya¹
Graduate School of Energy Science, Kyoto University, Uji, 611-0011, Japan
¹*National Institute for Fusion Science, Toki, 509-5292, Japan*
(Received: 9 December 2003 / Accepted: 1 April 2004)

Abstract

MHD equilibria of Heliotron J plasma are investigated by using HINT code. By assuming some profiles of the current density, effects of the net toroidal currents on the magnetohydrodynamics (MHD) equilibrium are investigated. If the rotational transform can be controlled by the currents, the generation of good flux surfaces is expected. In order to study equilibria with self-consistent bootstrap current, the Boozer coordinates are constructed by converged HINT equilibrium as a preliminary study. Obtained spectra are compared with ones of VMEC code and both results are consistent.

Keywords:

MHD, equilibrium, net plasma current, Boozer coordinate, Heliotron J

1. Introduction

Heliotron J device is an $L = 1/M = 4$ Helical-Axis Heliotron configuration, which has large flexibility [1]. The main parameters are $R = 1.2$ m, $\langle a_p \rangle \sim 0.1\text{--}0.2$ m, $B \leq 1.5$ T and $t \sim 0.4\text{--}0.8$, where R is the major radius, a_p is the averaged minor radius and t is the rotational transform. Heliotron J has a low shear and the magnetic configuration is very sensitive to the plasma pressure effect. In addition, since the effective toroidicity is not small, the Shafranov shift is large and the plasma shape is changed for finite β equilibria. Recently, finite β equilibria of Heliotron J plasma are studied by HINT [2] and PIES [3] codes. By using these codes, it was found that flux surfaces are broken by the magnetic island [4,5]. However, those study were based on the current-free equilibrium.

In recent Heliotron J experiments, the net toroidal currents are observed by the Rogowski coil [6]. These currents consist of the bootstrap, Ohkawa and electron cyclotron heating (ECH) currents. Effects of these currents on MHD equilibrium are very important, because properties of MHD equilibrium are strongly influenced by these currents.

In this paper, we study MHD equilibrium of Heliotron J plasmas more extensively. In particular, we investigate the generation of how to maintain good flux surfaces for the finite β equilibrium. This paper is organized as follows. In Sec. 2, the numerical scheme of the HINT code is reviewed briefly. In Sec. 3, we study finite β equilibria of the standard configuration in Heliotron J configuration. In addition, the effects of the vertical field and the net plasma currents are

studied. In the last section, we conclude the obtained results.

2. Numerical scheme of HINT code

HINT code is a three-dimensional equilibrium calculation code based on the time-dependent relaxation method, which uses non-orthogonal helical coordinates (u^1, u^2, u^3) . On this coordinate, the calculation is performed in following steps.

The first step (step-A) is a relaxation process to satisfy the condition $\mathbf{B} \cdot \nabla p = 0$. The relaxed pressure on a grid is given by the averaged pressure;

$$p \sim \bar{p} = \frac{\int p d//B}{\int d//B}, \quad (1)$$

which started from a grid point and uses it as update pressure on its grid. However, for low shear stellarator, field lines must be traced very long to obtain the relaxed pressure distribution and the computational time is consuming in this part. In order to resolve this technical problem, we introduce improved scheme of the pressure relaxation. The detailed description of the numerical scheme is referred to ref. [4].

The next step (B-process) is a relaxation of the magnetic field under the plasma pressure distribution is fixed. This process solves the time evolution of dissipative equations as follows;

$$\frac{\partial v}{\partial t} = -f_c[\nabla p - (\mathbf{j} - \mathbf{j}_0) \times \mathbf{B}], \quad (2)$$

$$\frac{\partial \mathbf{B}}{\partial t} = \nabla \times \left\{ \mathbf{v} \times \mathbf{B} - \eta \left[\mathbf{j} - \mathbf{j}_0 - \mathbf{B} \frac{\langle \mathbf{j} \cdot \mathbf{B} \rangle_{net}}{\langle B^2 \rangle} \right] \right\}, \quad (3)$$

$$\mu_0 \mathbf{j} = \nabla \times \mathbf{B} \quad (4)$$

where \mathbf{j}_0 is the external coil current. Brackets $\langle \dots \rangle$ indicates the flux surface average and $\mathbf{B} \langle \mathbf{j} \cdot \mathbf{B} \rangle_{net} / B^2$ is the net plasma current like Ohmic and neoclassical currents. The dissipative parameter η is assumed to be constant for equilibrium calculation. The factor f_c as,

$$f_c = \begin{cases} 1 & \text{for } |\mathbf{B}| \leq B_C \\ (B_C / |\mathbf{B}|)^2 & \text{for } |\mathbf{B}| > B_C \end{cases} \quad (5)$$

is calculated on all grid points, where $|\mathbf{B}|$ is the strength of the field and B_C is a critical value of the field strength. If there is a coil in the computation region, the Courant-Friedrichs-Levy condition (CFL condition) is very severe near a coil, because the Alfvén velocity is very fast due to the strong field

near a coil. By introducing f_c , the propagation velocity is uniform in the computational region and the CFL condition is satisfied.

The final equilibrium state is solved by these process iteratively until $d\mathbf{v}/dt \rightarrow 0$ and $d\mathbf{B}/dt \rightarrow 0$.

3. Effects of net plasma currents on MHD equilibrium

The ‘standard configuration’ of Heliotron J plasma is shown in Fig. 1. This configuration is the fundamental configuration in actual experiment. Radial profiles of the rotational transform and the magnetic well are also plotted. The profile of the rotational transform is flat ($t \sim 0.55$) and the magnetic well exists at the vacuum. Nested flux surfaces are maintained to edge region.

Poincaré plots of a finite pressure equilibrium for $\langle \beta \rangle = 0.4\%$ are shown in Fig. 2. The initial distribution of the plasma pressure are specified to $p = p_0(1 - s^2)^2$, where s is the normalized toroidal flux. The chain of magnetic islands is generated by the resonance $4/7$ (~ 0.57), because the rotational transform t on the axis is increased by the Shafranov shift.

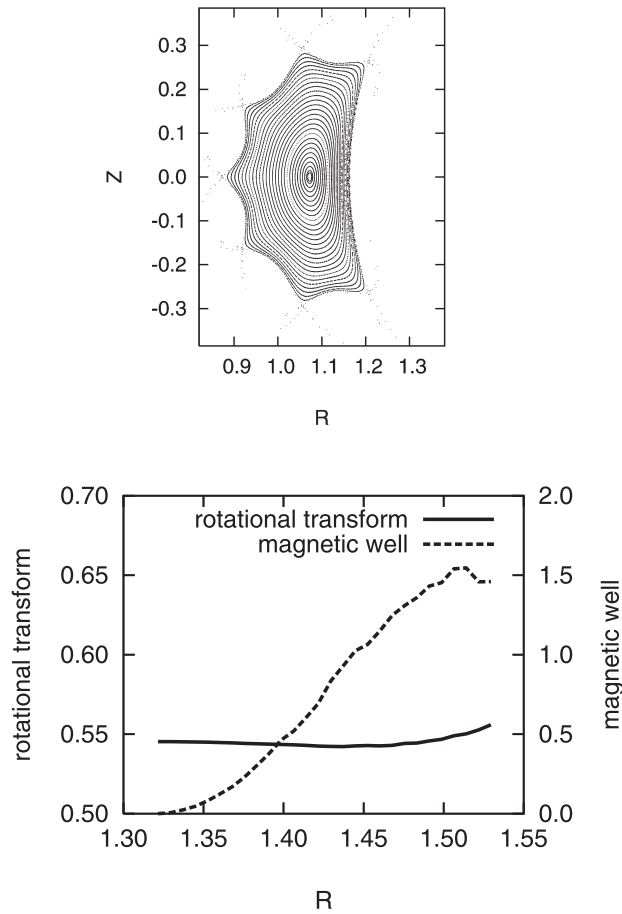


Fig. 1 Poincaré plots and radial profiles of the standard configuration are plotted. Flux surfaces are plotted at $M\phi = \pi$. The rotational transform and the magnetic well are plotted as the function of the major radius R at $M\phi = \theta = 0$.

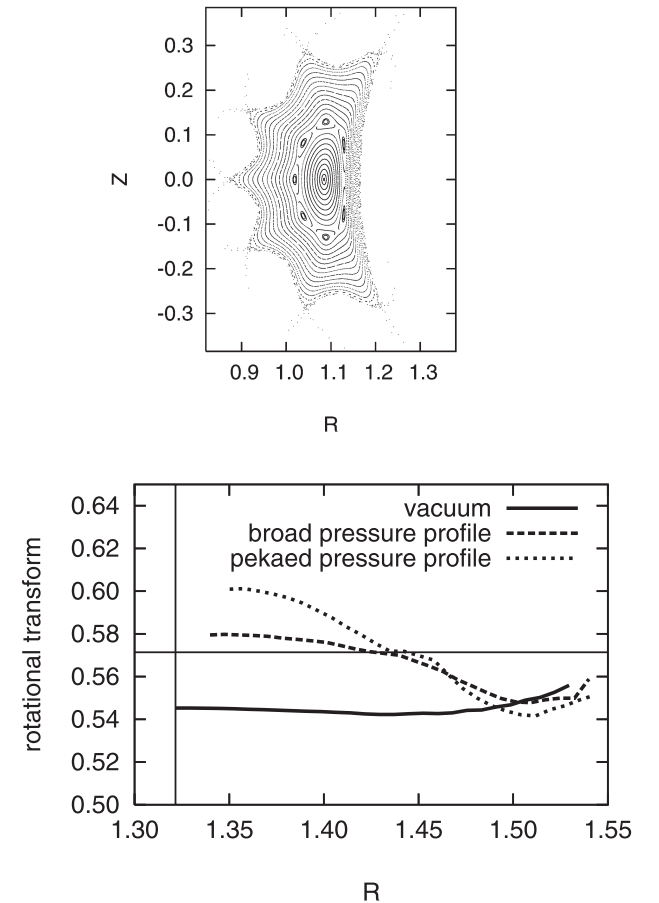


Fig. 2 Poincaré plots and radial profiles for finite β equilibria ($\langle \beta \rangle = 0.4\%$) with different pressure profiles are shown corresponding to Fig. 1. Flux surfaces are plotted for the broad pressure profile. The profile for the vacuum is also plotted for comparison. $R = 1.32$ line indicates the position of the axis for the vacuum and $t = 0.571$ line indicates $n/m = 4/7$.

These islands are grown due to the increased β . Profiles of the rotational transform with different pressure profiles are also shown. For the peaked pressure profile, since the Shafranov shift is large, t on the axis is increased as compared with the broad profile. However, the magnetic shear is large at $t = 4/7$ and the width of islands is not increased.

For Heliotron J configuration, the magnetic island is generated by the resonance of the rational surface, because the rotational transform is changed due to the Shafranov shift. If the rotational transform can be controlled by some kind method, the magnetic island can be suppressed. One of possibilities is the using the net plasma currents. In Heliotron J experiment, the net plasma currents ($\sim \pm 3$ kA) are observed by the diagnostic of the magnetic loops. By using these currents, it has possibility to control the rotational transform. The net plasma currents are driven by the neoclassical effects. If we would like to estimate these currents consistently, it is required to calculate the neoclassical transport. However, for helical system plasmas, it is difficult to estimate the neoclassical current consistently. Therefore, in this

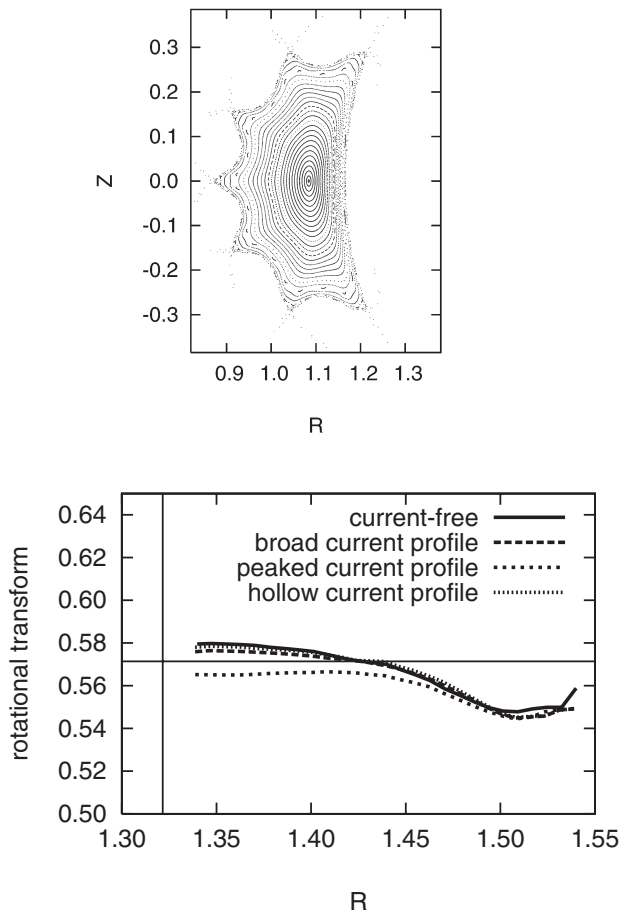


Fig. 3 Poincaré plots and radial profiles for finite β equilibria ($\langle\beta\rangle = 0.4\%$) with different current density profiles are shown corresponding to Fig. 1. Flux surfaces are plotted for a profile of the peaked current density. The profile for the current-free case is also plotted for comparison. $R = 1.32$ line indicates the position of the axis for the vacuum and $t = 0.571$ line indicates $n/m = 4/7$.

study, we study equilibria with the net plasma current prescribed to a profile as the function of the toroidal flux. Profiles of the current density in this study are shown as follows;

$$j = 2(1 - s^4)^2, \quad \text{peaked profile} \quad (6a)$$

$$j = (1 - s)^8, \quad \text{broad profile} \quad (6b)$$

$$j = 60(1 - s^2)s^2, \quad \text{hollow profile} \quad (6c)$$

where s is the normalized toroidal flux.

In Fig. 3, Poincaré plots and profiles of the rotational transform for equilibria with the net toroidal currents are shown. The rotational transform for the current-free case is also plotted for comparison. The volume averaged beta $\langle\beta\rangle$ is 0.4 % and the net toroidal current is fixed to 2 kA in the direction of 'negative'. The rotational transform on the axis is decreased and the Shafranov shift is hardly changed by the current. For the peaked current profile, the rotational transform becomes below $t = 4/7$. In Poincaré plots, good flux surfaces are maintained. However, high order rational surface $n/m = 12/22$ are shown and other rational surface will be generated for higher- β . These are increased due to the β value and the edge region is ergodized by these surfaces. For other two profiles, since the change of the rotational transform is very small, the magnetic island is not suppressed. On the other hand, for 'positive' current, the rotational transform on the axis is increased and the position of the resonance $4/7$ moves to outside surfaces. For the broad and hollow profiles, the width of the island is slightly increased as compared with the current-free equilibrium. However, for the peaked current profile, since the magnetic shear is strong at the resonance $4/7$, the width of islands is suppressed. The Shafranov shift is hardly changed as well as the negative current.

For analyses of the bootstrap current for helical system plasmas, the SPBSC code [7] is used on the Boozer coordinates in many cases. By combining VMEC and SPBSC code, the equilibrium with self-consistent bootstrap current can be obtained iteratively. We plan the study of the equilibrium including self-consistent bootstrap current by the above men-

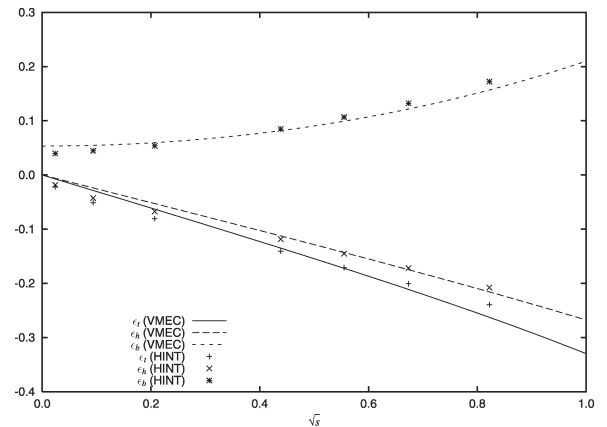


Fig. 4 Spectra of dominant components on the Boozer coordinates. Points indicate spectrum obtained from converged HINT equilibrium and lines indicate spectrum from VMEC. Both results are consistent.

tioned scheme. As a preliminary study, we construct the Boozer coordinates using the vacuum field as a very low- β equilibrium. In order to construct the coordinate, we adopt the scheme by Boozer *et al.* [8]. Figure 4 shows dominant components on the Boozer coordinates. Same spectra obtained from VMEC and NEWBOZ codes are also shown for comparison. Both results are in good agreement. However, our code can not yet construct the Boozer coordinate of the equilibrium with islands or stochastic regions automatically. We will resolve this difficulty using ‘quasi-magnetic coordinates’ [3].

4. Summary

Using HINT, we study properties of MHD equilibrium for the realistic β equilibrium. The magnetic island of Heliotron J plasmas is generated by the resonance of the rational surface, because the rotational transform reaches the resonant surface by the Shafranov shift. In order to generate good flux surfaces for finite β , effects of the net plasma current are studied under the condition which has the current density profile prescribed to the function of s . For equilibria with the net toroidal current, the Shafranov shift is hardly changed by the current but the rotational transform is changed. For the negative current with the peaked current profile, the rotational transform avoids the resonance $4/7$. However, a high order rational surface appeared. In actual

experiments, the currents driven by the neutral beam injection (NBI) are observed and the profile of the current density is expected to become the peaked profile. From this study, under realistic β , possibility of generation of good flux surfaces is found. In addition, as a preliminary study of the bootstrap current calculation by the SPBSC code, we construct the Boozer coordinate based on a HINT equilibrium. Generated harmonics is consistent to harmonics obtained by the VMEC code. Studies of the equilibrium with the bootstrap current are now in progress.

Acknowledgment

This work was done in the program in the 21st century of “Establishment of COE on Sustainable-Energy System” from the Japan Society for the Promotion of Science.

References

- [1] M. Wakatani *et al.*, Nucl. Fusion **40**, 569 (2000).
- [2] K. Harafuji *et al.*, J. Comput. Phys. **81**, 169 (1989).
- [3] A. Reiman *et al.*, Comp. Phys. Comm. **43**, 157 (1986).
- [4] Y. Suzuki *et al.*, Plasma Phys. Control. Fusion **45**, 971 (2003).
- [5] Y. Nakamura *et al.*, Nucl. Fusion **44**, 387 (2004).
- [6] H. Okada *et al.*, J. Plasma Fusion Res. *submitted*.
- [7] K.Y. Watanabe *et al.*, Nucl. Fusion **41**, 63 (2001).
- [8] G. Kuo-petravic *et al.*, J. Comput. Phys. **51**, 261 (1983).